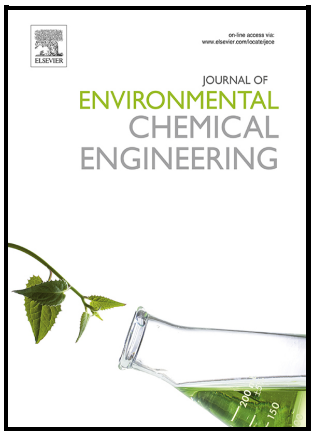

Two-step valorization of invasive species *Rosa rubiginosa* L. husk waste through eco-friendly optimized pectin extraction and subsequent pyrolysis

Rodrigo Torres-Sciancalepore, Mathias Riveros-Gomez, Daniela Zalazar-García, Daniela Asensio, María Paula Fabani, Rosa Rodriguez, Gastón Fouga, Germán Mazza

PII: S2213-3437(23)01541-5

DOI: https://doi.org/10.1016/j.jece.2023.110802

Reference: JECE110802

To appear in: *Journal of Environmental Chemical Engineering*

Received date: 5 May 2023
Revised date: 21 July 2023
Accepted date: 17 August 2023

Please cite this article as: Rodrigo Torres-Sciancalepore, Mathias Riveros-Gomez, Daniela Zalazar-García, Daniela Asensio, María Paula Fabani, Rosa Rodriguez, Gastón Fouga and Germán Mazza, Two-step valorization of invasive species *Rosa rubiginosa* L. husk waste through eco-friendly optimized pectin extraction and subsequent pyrolysis, *Journal of Environmental Chemical Engineering,* (2023) doi:https://doi.org/10.1016/j.jece.2023.110802

Two-step valorization of invasive species *Rosa rubiginosa* L. husk waste through eco-friendly optimized pectin extraction and subsequent pyrolysis

Rodrigo Torres-Sciancalepore[a,#], Mathias Riveros-Gomez[b,#], Daniela Zalazar-García[b], Daniela Asensio[a], María Paula Fabani[b], Rosa Rodriguez[b], Gastón Fouga[c], Germán Mazza[a*]

[a]Instituto de Investigación y Desarrollo en Ingeniería de Procesos, Biotecnología y Energías Alternativas, PROBIEN (CONICET-Universidad Nacional del Comahue), Calle Buenos Aires 1400, Neuquén (8300), Argentina

[b]Instituto de Ingeniería Química - Facultad de Ingeniería, Universidad Nacional de San Juan - Grupo Vinculado al PROBIEN (CONICET-UNCo), Av. Libertador San Martín (Oeste) 1109, San Juan (5400), Argentina

[c]Departamento de Fisicoquímica y Control de Calidad, Complejo Tecnológico Pilcaniyeu, Centro Atómico Bariloche, Comisión Nacional de Energía Atómica and Consejo Nacional de Investigaciones Científicas y Técnicas (CONICET), Av. Bustillo 9500, S.C. de Bariloche (8400), Río Negro, Argentina

*Corresponding author: german.mazza@probien.gob.ar (orcid.org/0000-0002-1362-8521)

#Rodrigo Torres-Sciancalepore and Mathias Riveros-Gomez have equal contributions

Abstract

This research studied chemical and thermal treatments of rosehip husk (RH), from invasive species in Patagonia *Rosa rubiginosa*, which is considered a main waste in the seed-oil extraction industry, to obtain added-value products by optimizing an eco-friendly pectin extraction, followed by pyrolysis of the remaining solid (RHW). The aim was to valorize the rosehip husk of an invasive species by finding the optimal conditions for pectin extraction (maximum yield and minimum CO_2 emissions) and assessing the pyrolysis process together with the products obtained, finding the temperature of maximum production of each species in the gaseous product. By applying multi-objective optimization, it was found that the optimal yield was 17.83 % with 456.7 g of CO_2 emitted for kg of pectin at temperature T = 79.6 ºC, time t = 30 min, and pH = 2.3. By TGA, 6 processes were identified in the pyrolysis of RHW: moisture evaporation and 5 consecutive reactions which were related to

lignocellulosic biomass components decomposition. The kinetic parameters of each reaction were obtained by isoconversional method (activation energy), compensation effect method (pre-exponential factor), and master-plots method (conversion function). The pyrolysis gaseous products of energetic interest identified were CH_4, H_2, and C_2H_4, with maximum production at 630, 700, 850 ºC respectively. The main compounds found by GC-MS were diacetone alcohol, mesityl oxide, butylated hydroxytoluene, among others. The ash was analyzed by XRD and showed a high Ca concentration (46.9 %) with presence of $Ca(OH)_2$, MgO, $KCaPO_4$, and $K_4Ca(PO_4)_2$.

Keywords: rosehip husk waste; pectin extraction optimization; invasive shrub species valorization; slow-pyrolysis products; biomass waste recovery; biomass to hydrogen.

1. Introduction

Rosa rubiginosa (commonly known as sweet briar or rosa mosqueta) is a shrub from the Rosaceae family native to Europe and Asia where it is widely distributed, although it can also be found in South America, Australia, and New Zealand as an exotic (non-native) species. The population of this species found in Patagonia (Argentina) has a close genetic similarity with the ones found in Germany, the Czech Republic, Austria, Italy, and Slovakia [1]. Due to its adaptive nature as a consequence of the efficient use of light, water, and minerals that allow *R. rubiginosa* to survive in extreme environments, it is considered a highly expansive species, giving it characteristics of an *invasive* species [2]. The expansive nature of *R. rubiginosa* endangers the regional ecosystem as some native plant species are displaced and extinct, producing changes in biodiversity and natural resources [3,4]. In

Argentina, *R. rubiginosa* is listed in Resolution No. 109/21 of the Ministry of Environment and Sustainable Development as a category II invasive exotic species, meaning that it is a species of controlled use, and can be utilized for productive or economic purposes.

R. rubiginosa rosehip is very commonly used to produce jams, infusions, soups, wine and additives from the husk, while oil is frequently extracted from seeds by cold pressing [5–7] for its pharmaceutical and cosmetic properties. Although the literature contains little information about where and how much fruit is produced, Quiroga [6] reported that the latest data collected from 2005 showed that about 55 % of global sweet briar production came from Chile and Argentina. Industries that produce only rosehip seed oil by cold pressing leave two main bio-wastes: the pressed seeds, and the rosehip husk (which is the dehydrated mature seedless receptacle). Therefore, it is of interest to look for alternatives for the valorization of the generated bio-wastes that currently cause problems in their final disposal, and thus also the associated environmental problems. This study then, proposes a two-step valorization of the rosehip husk through a pectin extraction followed by the pyrolysis of the remaining solid waste fraction.

A biorefinery is a type of refinery where biomass is treated in a production scheme based on the circular economy concept, in which all materials and wastes are reused and recycled regeneratively and restoratively [8]. The main challenge for biorefineries is the study of different alternatives for waste recovery or valorization, intending to achieve *zero waste* emissions, and maximum productivity and profits [8].

Many authors have proven the reduction of environmental impact and estimated the economic benefit of applying a biorefinery [9–12]. Zoppi et al. [13] applied the life cycle assessment (LCA) methodology to assess the environmental impacts of a biorefinery that

integrates hydrothermal liquefaction and aqueous phase reforming using corn stover and lignin-rich stream as possible feedstocks, allowing a 37% environmental impact reduction compared to fossil diesel, further reduced to 80% with the lignin-rich stream when green energy was used. Wang et al. [14] identified the integrated microalgal biorefinery as a possible solution for high-cost microalgal biofuel production, emphasizing the importance of integrating biorefinery with multiple routes for energy and economic advantages. Vignesh et al. [15], Malik et al. [16], and Haghpanah et al. [17] also used microalgae as feedstock to obtain a spectrum of products by applying a cascade biorefinery. Espinosa et al. [18] proposed the use of orange peel in a multi-component cascade approach to obtain polyphenolic compounds and nanocellulose. Yadav et al. [19] and Banu et al. [20] published a review of lignocellulosic biomass as a promising bioresource for the production of green fuels and biomaterials to promote the circular bioeconomy. Yadav et al. [19] showed that it is possible, through machine learning techniques in optimization and process control, to improve decision-making, resource exchange and knowledge discovery in sustainable biofuels production from biomass. A two-step biorefinery has been studied by Padilla-Rascón et al. [21] for the treatment of olive stone by dilute acid hydrolysis followed by an organosolv delignification, achieving a fully integrated usage of all biomass components. Ortiz-Sanchez et al. [8] proposed a biorefinery approach to producing essential oil, pectin, and biogas from orange peel waste. Sabater et al. [22] suggested possible uses of agri-food wastes in stages, starting with the recovery of compounds soluble in organic solvents such as polyphenols, carotenoids, and essential oils, followed by the pectin extraction, and the subsequent use of the spent residue in biofuels production by physicochemical or biological processes or its composting or animal feed.

A possible alternative to applying the concept of circular economy in the industrialization of rosehip fruit is the pectin extraction from the rosehip husk and subsequent pyrolysis process of the remaining solid, for the production of by-products with high economic value. Pectin is a complex polysaccharide with many industrial applications for their gelling, thickening, and adsorption properties. Chandel et al. [23] reviewed the current pectin extraction methods, properties, and their multiple applications: food industry (jams and jellies, emulsifying agents, bakery products, prebiotic properties and stabilizing acidified milk products), packaging industry (food packaging film and food coating), and pharmaceutical industry (reduction in LDL cholesterol in plasma, antioxidant activity, metal binding properties, glycemic control, encapsulating agent, and therapeutic and pharmaceutical uses). The traditional pectin extraction method consists of immersing biomass in an inorganic acid solution assisted by agitation and temperature, allowing the hydrolysis process to occur [24]. Ultrasound-assisted extraction considerably improves cellular compound diffusion, reducing the extraction process time to approximately one-third [25]. A combination of ultrasound and an organic acid solution provides a cleaner, less expensive pectin extraction procedure with promising results [26]. Different authors have studied the valorization of biomass waste by pectin extraction. Pedraza-Guevara et al. [27] established a sustainable protocol for extracting pectin from discarded unripe papaya. Kute et al. [28] analyzed the effect of microwave and acid extraction on pectin characteristics from orange peel powder. Zhu et al. [29] indicated that pectin extracted from Crataegus pinnatifida, which belongs to the *Rosaceae* family as does *R. rubiginosa*, is a low-molecular-weight pectin with potential applications for the food and pharmaceutical industry.

After pectin extraction, a residual solid fraction remains that may still be treated to obtain value-added products. One of the main alternatives is the thermochemical route, which can be divided into three main possible processes: pyrolysis, gasification, and combustion [30]. Pyrolysis is a thermochemical process under an inert atmosphere, in which the biomass (or other feedstock) is transformed into value-added products and energy. For industrial purposes, it is essential to fully characterize the reactions involved and the products obtained before designing pilot plant reactors. The reactions involved in pyrolysis processes are highly dependent on the molecular composition of the biomass. Different authors have modeled the pyrolysis process considering three main reactions following the decomposition of the three main constituents of lignocellulosic biomass: hemicelluloses, cellulose, and lignin [31–33]. The products obtained from biomass pyrolysis may be categorized into three types: biogas, bio-oil, and biochar. Biogas is the gaseous fraction of the products, composed mainly of light hydrocarbons, hydrogen, carbon monoxide, and carbon dioxide. The volatiles that condense at ambient temperature (except for water) are commonly known as bio-oil constituents and are generally hydrocarbons, phenolic, and other aromatic compounds. Different value-added compounds of interest may be obtained by distillation from bio-oil. Biochar is a solid-phase carbonaceous product consisting of fixed carbon and ash. It is mostly used for environmental purposes, such as soil amendment, for its adsorption characteristics [34,35]. Biochar is also a feedstock for combustion processes in energy plants or gasification processes for obtaining syngas. Additionally, kinetic data of the pyrolysis reactions is fundamental for the design of the reactors in a biorefinery.

The objective of this work is to study a two-step biorefinery around *R. rubiginosa* rosehip waste: an eco-friendly pectin extraction from the rosehip (RH) followed by the slow pyrolysis

of the remaining waste (RHW). The possibility of giving added value to the rosehip of *R. rubiginosa* husk by pectin extraction or pyrolysis has not been previously studied and poses an attractive alternative for the regional economy. Therefore, the aim was put into finding the maximum yield of pectin, minimizing CO_2 emissions as much as possible, as well as finding the optimal pyrolysis temperature for the species obtained in the gaseous product, among which methane, ethylene and hydrogen are highlighted since they are of energy interest. Pyrolysis (and pyrolysis products) study is of interest as a prior step to gasification process, to enhance the gas production, especially considering that biochar gasification with CO_2 does not start until 850/900 °C for this biomass. To characterize the pyrolysis reactions and the multiple products obtained (being of great importance for the development of a pilot plant and subsequent operation of industrial reactors) different analysis techniques were used, including thermogravimetry, infrared spectroscopy, gas chromatography, mass spectroscopy, scanning electron microscopy and X-ray diffraction. So far, no reports on pectin extraction from rosehip husk from *R. rubiginosa* have been found that demonstrate multi-objective optimization considering both process yield and CO_2 emissions as decision variables. This study proved that this residue is a promising source of this by-product with high economic value and multiple applications, highlighting the utilization of alternative and eco-friendly extraction technology. Furthermore, it is the first work on the complete use of rosehip husk in two steps (pectin extraction and pyrolysis), aiming to implement the concept of circular economy and zero waste to the industrialization processes of the rosehip from an invasive species.

2. Materials and methods

Fig. 1 shows a scheme of this work showing the two steps carried out: the optimization of pectin extraction from RH and the pyrolysis experiments that were performed on RHW.

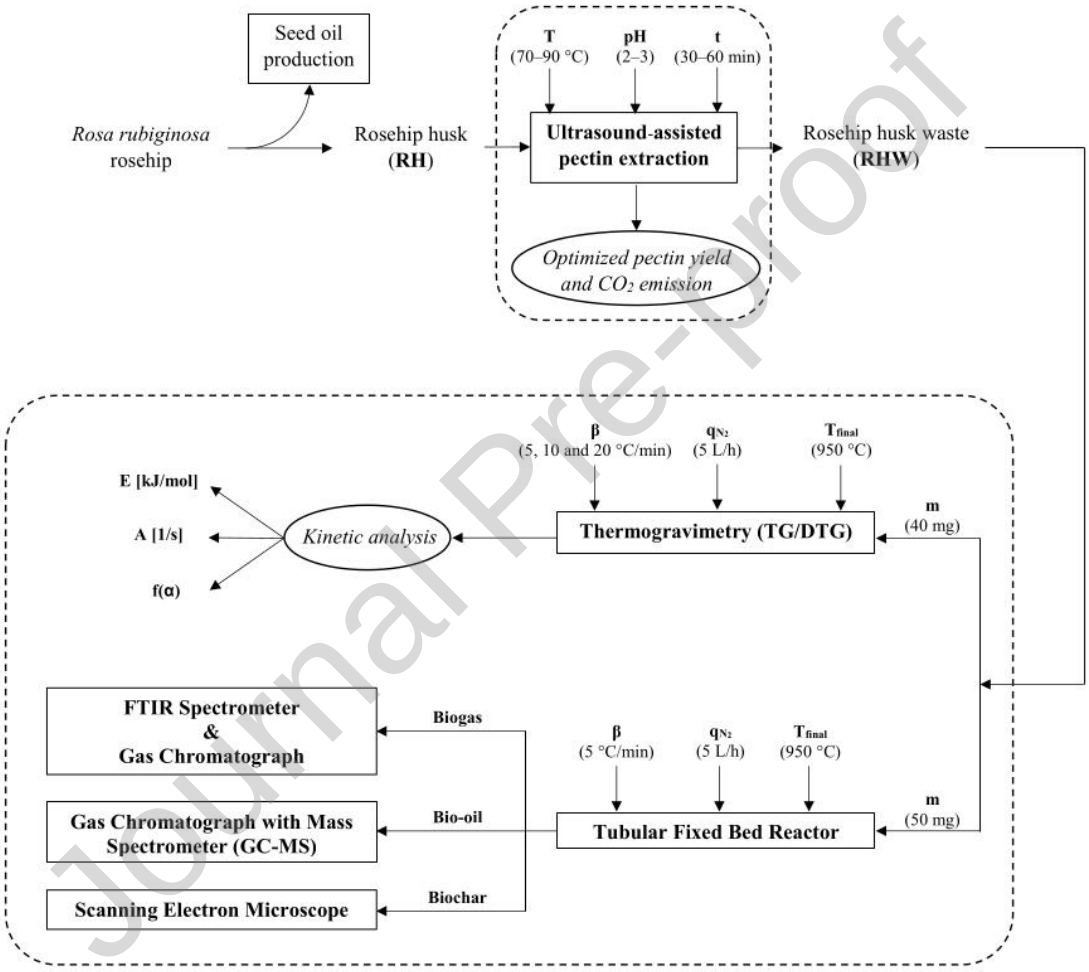

Fig. 1. Logic diagram of valorization of *Rosa rubiginosa* L. husk. in two steps

2.1 Materials

Rosehip fruits were collected in the city of San Carlos de Bariloche, Rio Negro, Argentina, (41°3'39.24"S; 71°33'59.4"W) in March (which is the harvest month). They were dried at

70 °C for 24 h in a free convection oven (San Jor SL30SDB), having previously made three or four perforations on the fruits to allow moisture to escape. The dried fruit husk was separated from the seed, ground to low granulation, and stored in plastic bags with double zippers for subsequent use.

2.2 Rosehip husk characterization

RH samples were chemically characterized by determining moisture (AOAC method 925.10), lipids (AOAC method 920.39: Soxhlet extraction), proteins (AOAC method 960.52: Kjeldahl method), ashes (AOAC method: 923.03: by calcination at 580 °C until white ashes are obtained), and crude fiber (AOAC method: 962.09), as well as Klason lignin (standard method ASTM D1106), cellulose (standard method ASTM D1103), holocellulose (method proposed by Browning [36]), and hemicellulose (by difference between cellulose and holocellulose). The following physicochemical parameters were evaluated: pH (AOAC method 10.042), titratable acidity (AOAC method 942.15), and solid soluble content (AOAC method 932.12). After pectin extraction, an exhausted solid waste (RHW) was obtained and dried at 70 ºC for 24 h. The same characterization carried out in RH was made in RHW to infer the effect of the extractive process on the composition and physicochemical properties of solid residue. On the other hand, the RHW fraction was subjected to slow pyrolysis to study the thermochemical characteristics of the waste decomposition.

Before the pyrolysis experiments, RHW particle size distribution was determined by laser diffraction analysis in a particle-size analyzer (Cilas 1190) with a particle size detection range of 0.04 µm to 2500 µm. Before measuring size distribution, the sample was immersed in an ultrasonic cell for 60 s in water to break up solid aggregates.

In addition, the higher heating value (HHV) of RHW was measured using an oxygen bomb calorimeter (1224 Parr) according to standards ASTM D 240-64 and ASTM D 271-70, while the lower heating value (LHV) was determined by Eq. (1) [37]:

$$\mathrm{LHV} = \mathrm{HHV} - 2.454\ (\mathrm{MO}/100 + 9 \times \mathrm{H}/100) \quad (1)$$

where MO is the moisture content of the RHW sample, and H is the hydrogen content, both expressed as percentages. H was determined with a Carlo Erba-Fisons EA 1108 automatic elemental analyzer.

Finally, to study the thermal decomposition characteristics of RHW, the volatile matter (VM) percentage was determined according to ASTM E872-82, while fixed carbon (FC) was calculated by difference (considering moisture and ash percentages previously determined).

2.3 Pectin extraction process

2.3.1 Experimental design, yield, and CO_2 emissions calculation

The pectin extraction process consisted of mixing the RH samples with a citric acid solution and submerging them in an ultrasound bath (Arcano brand, PS10-A model, 2 L capacity) at different residence times and temperatures. The traditional method consists of stirring the samples for 2 - 4 hours in inorganic acid solutions such as nitric, sulfuric, or chlorhydric [38,39]. Using an organic solvent and assisting the process with acoustic energy makes this process more eco-friendly and less expensive than the traditional extraction method.

The extraction technique was proposed by Riveros-Gomez et al. [26] and consists in placing samples (0.5 ± 0.001 g) in Falcon tubes with screw caps. The citric acid solution was added

to the tubes in a 1/25 g/mL mass/volume ratio and they were placed in the ultrasound bath, previously heated at a specific temperature, during the corresponding time. Then, tubes were centrifuged and samples were filtered to separate the liquid phase from RHW. Pectin precipitation was carried by adding 5 mL of ethanol (96 %) and tubes were refrigerated at 4 °C for 24 h to improve the gelling of pectin. Finally, pectin was filtered.

The Box-Behnken model design (BBD) [40] was applied, and the minimum and maximum experimental values for the independent variables were: pH (2–3), temperature (70–90 °C), and time (30–60 min), the range of these variables was chosen based on the reported by other authors and considering these points: i) Obtaining citric acid solutions with a pH less than 2 significantly increase de citric acid consumption (383 g of citric acid per liter of solution is required to reach pH 1.45, being this the lowest possible considering acid solubility at 25 °C); ii) higher temperatures increase the pectin solubility in the citric acid solution; iii) ultrasound-assisted extractions reduced time considerably considering the traditional method [41].

The extraction yield (η) was calculated according to Eq. (2). All the assays were performed in triplicate for each condition established in the experimental design.

$$\eta(\%) = (\text{dried pectin}/\text{dried sample}) \times 100 \quad (2)$$

The CO_2 emission was calculated based on energy consumption estimation at each one of the points of the experimental design. Two types of energy are associated with the ultrasound extraction process: the energy required to keep the bath at the specified temperature (E_h), and

the acoustic energy used in the ultrasound bath (E_u). The total electricity consumption (E_t) is determined as the sum of E_h and E_u.

E_h [kJ/kg of pectin] was calculated with Eq. (3):

$$E_h = (P_h \times t_h \times 100)/(\eta \times m) \quad (3)$$

where P_h is the heat power used by the equipment (50 W), m is the RH mass [kg], and t_h is the time the heater is on. E_u [kJ/kg of pectin] was calculated with Eq. (4):

$$E_u = (P_u \times t_u \times 100)/(\eta \times m) \quad (4)$$

where t_u is the extraction time and P_u is the appropriate ultrasound power (70 W) for reaching high pectin yields [42].

CO_2 emissions were indirectly calculated using a factor proposed by Transparency Climate [43]. As can be seen in Eq. (5), in Argentina this factor is equal to 358.3 g CO_2/kWh (Eq. 5):

$$CO_2 \text{ emission} = 358.3 \ \frac{g}{kWh} \ x \ E_t \quad (5)$$

It is important to note that the current study estimated extraction process CO_2 emission using laboratory data, but electricity and heat demands may differ in a large-scale procedure. It is assumed that comparable or better values of process yields may be obtained from a scaled-up process working under ultrasound intensity and energy-dissipation conditions similar to

those in a laboratory [44]. The energy effectively taken up by the samples was considered equal to 0.80 according to Prado et al. [45].

The BBD was used to model the process by fitting the η and CO_2 emission with a second-order equation (Eq. (6)) and to find the optimal value of factors and their interaction. The variation of dependent variables was analyzed using multivariate regression [46].

$$\hat{z} = b_0 + \sum b_i x_i + \sum b_{ij} x_i x_j + \sum b_{ii} {x_i}^2 \quad (6)$$

where $\hat{z}$ is the objective variable estimation, x_i and x_j are the independent variables considered in the model, while b_i, b_j, and b_{ij} are the regression parameter estimators.

2.3.2 Optimization of the pectin extraction process

Pectin extraction yield and CO_2 emission functions obtained were used to make a multiobjective optimization to find acceptable solutions that minimize the CO_2 emission and maximize the yield of the extraction. The procedure described by Riveros-Gomez et al. [26] was applied to optimize the objective functions (yield and emissions simultaneously).

2.3.3 Pectin quality

Some quality parameters of the extracted pectin were determined: water activity (a_w), ash content, equivalent weight (EW), methoxyl content (%Me), and degree of esterification (DE) [47,48]. Each test was performed in triplicate.

2.4 Pyrolysis experiments

2.4.1 Thermogravimetric and kinetic analysis

To study the decomposition of RHW with temperature throughout the pyrolysis process, thermogravimetric analysis (TGA) was performed in an STA 409 NETZSCH brand thermobalance using a heating program consisting of three different linear ramps at $\beta = 5$, 10 and 20 ºC/min from 20 ºC to 950 ºC, and a nitrogen flow rate of 5 L/h in all cases. The test was performed with an RHW sample mass weighing approximately 40 mg. Before measuring the sample, a blank was performed under the same conditions for background correction. The mass (m) vs. temperature plot (TG) is presented in the results section. The derivative thermogravimetric (DTG) curve with respect to time (t), which is the plot of dm/dt vs. temperature (T), was obtained by numerical differentiation using second-order Lagrange interpolating polynomials.

Different parallel processes were isolated from thermogravimetric data by deconvolution of the derivative curve of the conversion ($\alpha = (m_0 - m_t)/(m_0 - m_\infty)$) with temperature ($d\alpha/dT$) [49–51]. Lorentz function was selected for peak fitting of $d\alpha/dT$ since it presented the best results, and the Levenberg-Marquardt method was used for iteration. For each parallel reaction found, the kinetic parameters were determined following the methodology previously described by Torres-Sciancalepore et al. [49,52]: the activation energy (E) was determined by isoconversional methods, the pre-exponential factor (A) by the kinetic compensation effect, and the conversion model ($f(\alpha)$) by the master-plots method.

The isoconversional method was applied following the Kissinger-Akahira-Sunose (KAS), Flynn-Wall-Ozawa (FWO) and Starink approximations for the temperature integral [49–51,53,54]. The best approximation was selected by comparing the coefficient of

determination, the mean squared error, and the absolute average deviation. The coefficient of variation was calculated to observe the variability between the activation energy results with conversion.

The kinetic models considered for the kinetic compensation effect and master-plots methods for the estimation of the pre-exponential factor and conversion function are enlisted in the Supplementary Material, Table S1.

2.4.2 Fixed bed pyrolysis experiments and volatile product analysis

To study the pyrolysis products of RHW, the reaction was also carried out in a fixed-bed reactor. The installation consisted of a 65 cm-long cylindrical silica glass reactor inserted in an electric oven connected to a Dhacel CD101 temperature controller. Approximately 50 mg of the RHW sample was placed in a silica glass crucible inside the reactor, which was purged with 5 L/h of nitrogen for 90 min before heating until an inert atmosphere was reached. The sample was then heated at a rate of 5 °C/min from 20 °C to 950 °C with constant nitrogen flow. This temperature range was selected in order to visualize the possible maximum production of the different species in the gaseous product.

The reactor outlet was connected to a Perkin Elmer Spectrum 400 FTIR spectrometer with sodium chloride cell windows for the identification of the gaseous species released during the reaction, obtaining a semi-continuous spectrum from 20 ºC to 950 ºC. Additionally, a Gas Chromatograph SRI Instrument Model 8610C with a thermal conductivity detector (TCD) was used to detect hydrogen (H_2) from the pyrolysis gaseous product. The gases were extracted with a syringe every 10 min (50 °C) and injected into the chromatographic column (Alltech Column CTR I (1.82 m × 0.63 cm)).

In addition, the condensable liquid product (bio-oil) retained in the reactor outlet was dissolved with HPLC grade Sigma Aldrich acetone for subsequent analysis by GC-MS. A volume of 1 µl of the solution was injected into the gas chromatograph (Clarus 680) connected in series with a mass spectrometer (Clarus 600T Perkin Elmer). TurboMass Version 5.4.2.1617 (Perkin Elmer) was used for data acquisition. NIST/EPA/NIH Mass Spectral Library (version 2.0f) was used with NIST Mass Spectral Search software to identify the separated compounds.

Additionally, another silica glass reactor was used to determine the gas and liquid yields of the pyrolysis carried out under the same conditions (N_2 flow rate = 5 L/h; T = 950 °C; β = 5 °C/min). The reactor, which was oriented vertically with the nitrogen gas flowing upwards, containing the crucible with the biomass sample, was packed with alumina ceramic beads and a cooling coil to allow the condensable volatiles to condense inside the reactor. By weighing the reactor before and after pyrolysis occurred, it was possible to determine the incondensable gas mass that was produced (gas yield). Discounting the biochar weight in the crucible, the liquid yield was therefore calculated.

2.4.3 SEM-EDS and XRD analyses of solids

The raw RHW biomass, combustion ash of RHW at 950 ºC, and biochar obtained by pyrolysis of RHW in the fixed-bed reactor (Section 2.4.2) were analyzed with a scanning electron microscope (FIB-SEM Carl ZEISS Crossbeam 340) at 100 X and 1000 X to analyze the surface of the particles. Additionally, an EDS analysis of the samples was performed to semi-quantitatively determine their elemental composition with the FIB-SEM Carl ZEISS

Crossbeam. Finally, the composition of the ashes was analyzed by X-ray diffraction (XRD) using a Bruker Advance D8 diffractometer.

3. Results and discussion

3.1 Rosehip characterization analysis

Table 1 shows the physicochemical characterization of RH and RHW.

Table 1. RH and RHW physicochemical characterization.

Property	**RH**	**RHW**
moisture content [%]	2.96 ± 0.67	9.11 ± 0.71
pH	3.83 ± 0.04	2.77 ± 0.03
titratable acidity [%]	0.54 ± 0.02	0.78 ± 0.04
soluble solids [°Brix]	3.17 ± 0.12	2.77 ± 0.15

Comparing RH and RHW samples, titratable acidity increased as a consequence of the immersion in the citric solution, and pH therefore decreased. It is important to note that the acid pH of RH favors pectin extraction. The soluble solids content is lower in RHW, which may be due to the dilution of the free sugars in the solution. Soluble solids provide a measure of the sugar content in the rosehip, which consists mainly of glucose and fructose [55]. Some authors have reported similar values for the physicochemical parameters determined in the RH samples [56,57].

Table 2 shows the proximal composition of the rosehip husks before and after the pectin extraction process. RH is biomass composed mainly of lignocellulose, fiber, ashes, and proteins. Few reports on the composition of rosehip were found in the literature. Cañulaf et

al. (2022) found similar values for protein and ash, but the lipid contents determined in our samples were lower. It is possible to confirm that RH has a high ash content, as a consequence of its mineral composition which consists mainly of calcium, potassium, magnesium, and phosphorus [55]. RH and RHW are rich in lignocellulosic compounds and fiber. No report of the lignin, cellulose, and hemicellulose contents for this biomass was found in the literature.

Table 2. RH and RHW percentage proximal composition and lignocellulosic content on a dry basis.

Component	**RH**	**RHW**
lipid	0.41 ± 0.06	1.56 ± 0.11
protein	3.27 ± 0.25	3.52 ± 0.26
ash	6.35 ± 0.07	3.74 ± 0.01
crude fiber	12.06 ± 0.83	18.78 ± 0.54
lignin	26.04 ± 0.18	27.19 ± 0.93
cellulose	22.70 ± 0.53	28.91 ± 1.03
hemicellulose	5.99 ± 0.57	13.01 ± 0.19

The FC and VM of RHW were 23.34 ± 0.57 % and 72.92 ± 0.93 %, respectively. This FC value was relatively higher than for other biomasses [58], making pyrolysis a good alternative for biochar production [59]. VM and FC were similar to those for residues such as pine cone leaf, nectarine stone, and peach stone [58]. High VM values are desirable for bio-oil and biogas production [59], making RHW a good alternative for their production as well. The heating values of RHW (HHV = 16.96 ± 0.17 MJ/kg and LHV = 15.31 ± 0.13 MJ/kg) were higher than for many other biomasses such as chestnut shells, apple waste, and rice husk [58].

Laser diffraction analysis showed that RHW particle sizes ranged from 0.3 µm to 600 µm, although only 10 % of particles were smaller than 16.4 µm and 10 % were larger than 256.37 µm, while mean particle size was 113.95 µm. Fig. S1 in the Supplementary Material shows the full particle size distribution histogram.

3.2 Pectin extraction process modeling and optimization

In this study, RH was used as raw material for pectin extraction. Extraction yield and the associated CO_2 emission were studied considering as independent variables: Temperature (T), time (t), and citric acid solution pH (pH). It is interesting to note that there are few reports on rosehip pectin extraction, which is an interesting area of study.

The experimental value of extraction yield and the CO_2 emission estimated were adjusted to a second-order polynomic function using the BBD, in Table S2 (see Supplementary Material) the experimental and adjusted values at each experimental condition are detailed. Multivariable regression was applied, and ANOVA was performed using the Fisher's test to confirm the experimental data adjustment to the regression models. Table S3 in the Supplementary Material shows the ANOVA results. The *F* value calculated: 37.15 and 931.65 for pectin yield and CO_2 emission, respectively, were higher than the tabulated value (F (9,29,0.05) = 2.22), validating the model's adjustment for both pectin yield and CO_2 emission. On the other hand, the coefficients of determination (R^2) were 0.920 and 0.996 for pectin yield and CO_2 emission respectively, which are higher than 0.75, indicating a good model fit [60].

All model terms – constant, linear, and quadratic – were analyzed statistically using the *p* values (associated with the Student's *t*-test). When the *p*-value was higher than 0.05 (the

significance level considered was 95 %), the effect of this coefficient was "non-significant", which meant that the term analyzed did not contribute significantly to the dependent variable adjusted by the model, and was therefore dismissed. The Pareto chart (Fig. S2, Supplementary Material) shows the *p* values for each model term, and Table S4 in the Supplementary Material shows all the statistical parameters considered. Eqs. (7) and (8) are the mathematical expressions for pectin yield and CO_2 emission, respectively, considering the significant regression parameter estimators only:

$$\eta[\%] = -272.000 - 52.200\ \mathrm{pH} + 1.929\ \mathrm{t} + 7.650\ \mathrm{T} + 25.550\ \mathrm{pH}^2 - 1.132\ \mathrm{pH\ T} - 0.015\ \mathrm{t\ T} \quad (7)$$

$$\mathrm{CO_2\ emission\ [g\ CO_2/kg\ pectin]} = -331.000 + 5.250\ \mathrm{t} + 12.230\ \mathrm{T} - 0.020\ t^2 - 0.047\ \mathrm{T}^2 \quad (8)$$

The complete models, including de non-significant terms, are provided in the Supplementary Material, Eqs. (S1) and (S2).

Fig. 2 shows the response surface plots for pectin yield and CO_2 emission models for the independent variables considered in this study by pairs, fixing the third variable at its optimal value. As many authors have reported, the extracted pectin yield from different sources is favored by increasing T and t and reducing the hydrolytic solution pH [47,61,62]. However, higher T and longer t, increase the energy consumed in the process as well as the CO_2 emission of the process. As may be observed in Fig. 2 pectin yield may reach values higher than 35 % but with significantly higher CO_2 emission.

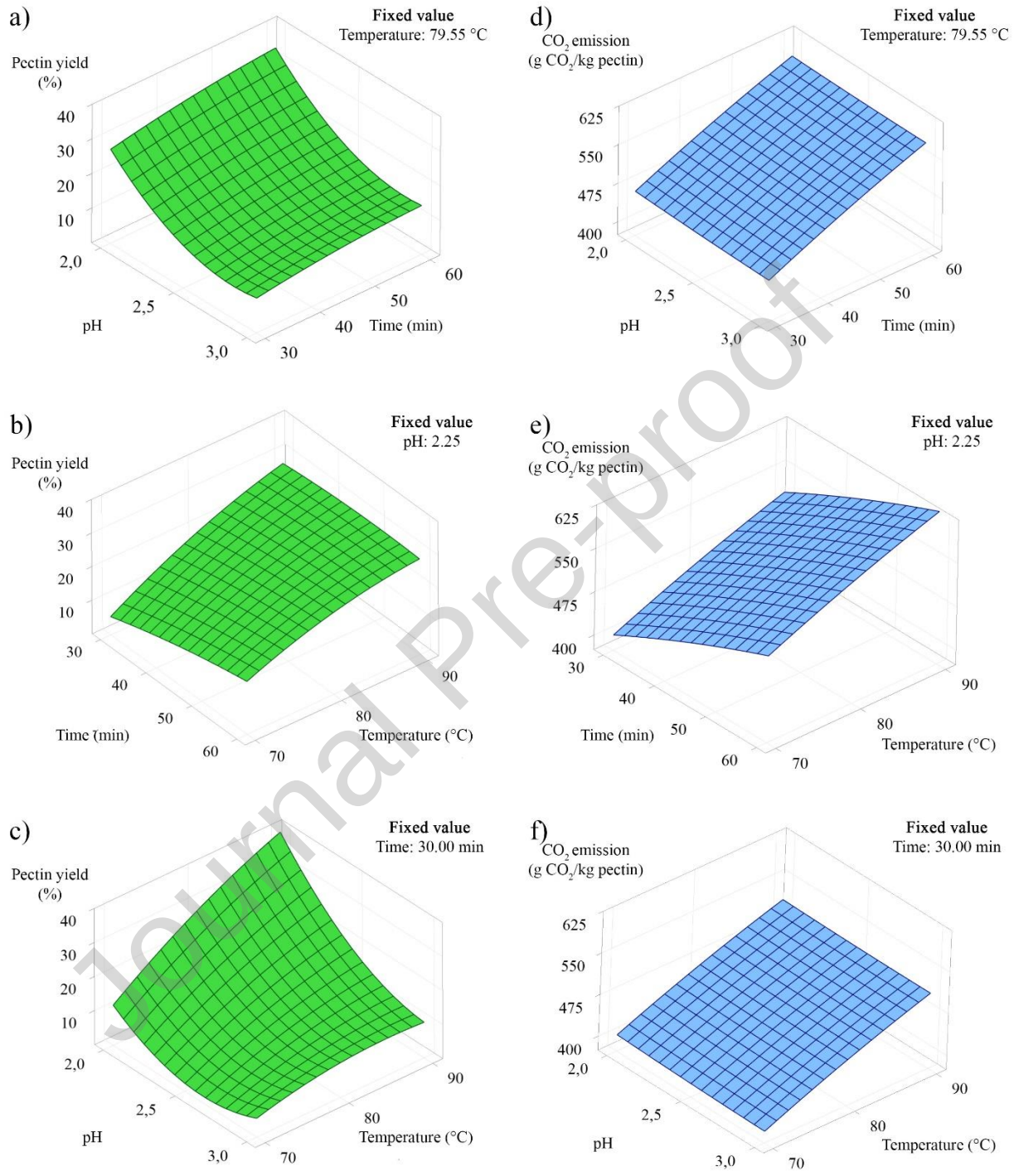

Fig. 2. Response surface plot of a) pectin yield vs. time and pH, b) pectin yield vs. time and temperature, c) pectin yield vs. pH and temperature, d) CO_2 emission vs. time and pH, e) CO_2 emission vs. time and temperature, and f) CO_2 emission vs. temperature and pH.

Reports of CO_2 emissions from ultrasound-assisted and the conventional extraction method of pectin extraction were not found in the literature. Acceptable solutions for decision-making can be found by applying multi-objective optimization. The Pareto front (Fig. S3 in the Supplementary Material) shows some of the optimization results. Analysis of the results shows that the most acceptable compromise solution corresponds to the following extraction conditions: T = 79.6 °C, pH = 2.3, and t = 30 min, through which a 17.83 % pectin yield is obtained with emissions equal to 456.7 g CO_2/kg pectin. The optimum pectin yield obtained from RH was 17.83 %, which is higher than the values reported by Taneva et al. [63], who used ammonium oxalate and stirring for pectin extraction from rosehip fruits, and by Ognyanov et al. [64] using a citric acid solution and stirring, obtaining a pectin yield of 13.01 % and 3.20 %, respectively. According to the literature, overall the pectin extraction yield through conventional methods from citrus peel and apple pomace ranges between 15–30 %, and 10–15 % respectively [65–67].

Ultrasound-assisted extraction is an eco-friendly technology that considerably improves the yield of the extraction and reduces processing time by approximately threefold because the acoustic energy enables the acid solution to penetrate cell walls easily, rupturing them and releasing pectin [41].

3.2.1 Pectin quality

Some quality parameters were measured in the RH pectin obtained under optimal conditions. Reducing a_w contributes to extending product shelf life. For pectin extracted from RH, a_w is 0.55 ± 0.01. The minimum a_w for all microbial growth is 0.60, while beneath this value, it is considered that if the product deteriorates, it is not due to microbiological reasons [68]. Ash

content lower than 10 % indicates that pectin quality is good for gel formation [48]. The ash content in RH pectin was 3.13 ± 0.04 %, which can be considered low. The EW was 281.00 ± 9.31 g/ml, which is similar and even higher compared to the values reported in the literature, indicating that the pectin structure was not degraded during the extraction process and maintained its absorption properties [47]. The %Me ranged from 0.2 to 12 % (4.42 ± 0.22 %), which indicates that RH pectin forms firm, stable gels [26]. Finally, pectin can be classified as low methoxyl pectin (LMP) when DE < 50 %, and high methoxyl pectin (HMP) when DE > 50 %. In RH pectin, DE was 28.59 ± 0.78 %, being then classified as LMP. The mechanism of gel formation in LMP is different from HMP as hydrogen bonding is absent, and the intermolecular bonding occurs through the formation of dimmers, using divalent cations, such as Ca^{+2}, Fe^{+2} and Zn^{+2}, thus forming cross-linking, using two carboxylic groups. The low methoxyl pectin forms gels at a higher pH in the range of 3 to 7, and the addition of sugar is then not necessary for gel formation [23,69].

3.3 Thermogravimetric analysis and kinetic parameters of RHW pyrolysis reactions

Fig. 3 shows the results of the thermogravimetric analysis: TG and DTG curves. The TG curve shows that the total mass loss throughout the heating program was approximately 80 % (depending on the heating rate) and that the global process of biomass disintegration occurs in multiple parallel processes. This is reflected in the TG curve by the changes in slope with increasing temperature or, more noticeably, in the DTG curve as overlapping peaks. The DTG curve enabled the identification of six peaks representing different processes that occur during RHW pyrolysis, marked from R1 to R6 in Fig. 3. The temperatures of the maximum decomposition rate of the six processes identified were around $T_{m1} \approx 90$ ºC, $T_{m2} = 201$ ºC,

T_{m3} = 236 ºC, T_{m4} = 333 ºC, T_{m5} = 409 ºC and T_{m6} = 691 ºC. The slight shift of the thermogravimetric curves towards higher temperatures with the heating rate (especially observed in the DTG curve) is related to a heat transfer delay that produces a difference between the actual temperature inside the sample and the one indicated by the temperature controller [70]. The first process, R1, at around 90 ºC, may be related to the evaporation of remaining moisture in the biomass.

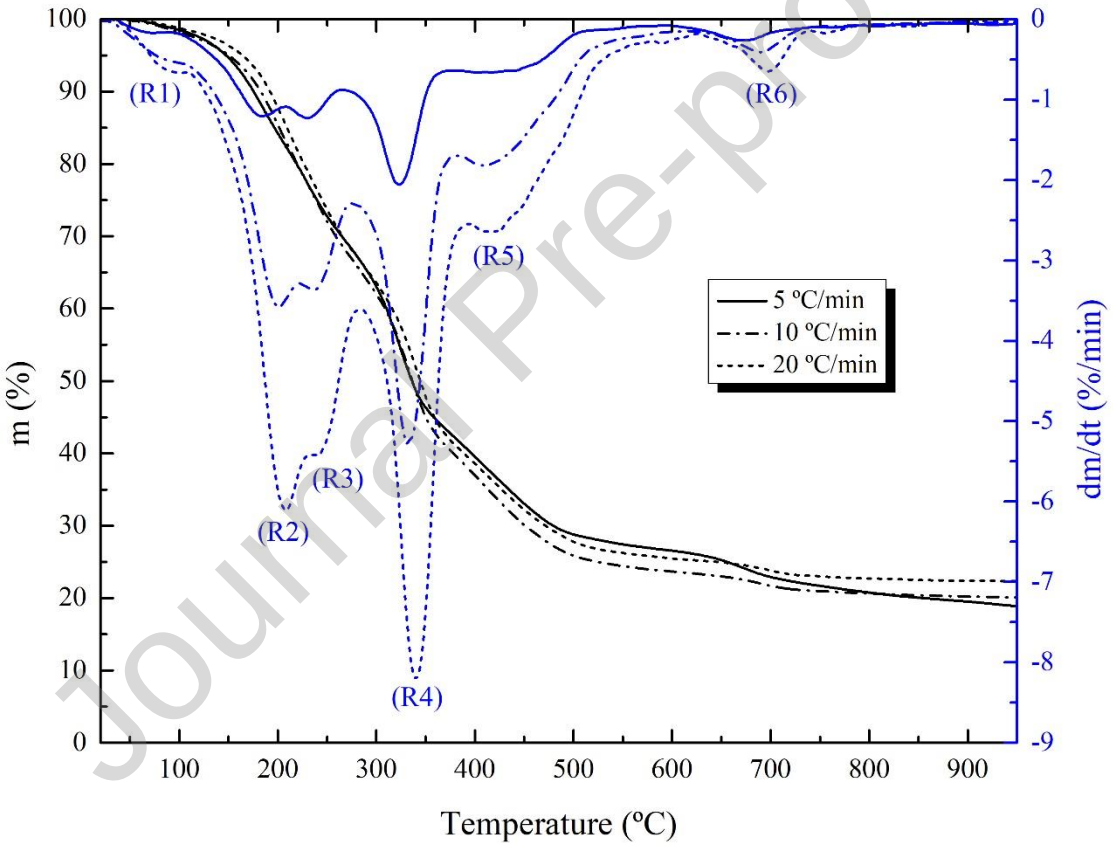

Fig. 3 Thermogravimetric results (TG/DTG) of RHW pyrolysis.

The second and third peaks, corresponding to processes R2 and R3, could be related to the decomposition of some light extractive compounds or hemicelluloses, polymers of monoses of five and six carbons present in lignocellulosic biomass. Aburto et al. [71] reported that

pectin decomposition by pyrolysis presents a maximum rate at approximately 200 °C, therefore, the process R2 may be related to the decomposition of a pectin fraction that may not have been completely extracted. Alternatively, some researchers, such as Chen et al. [33], Stefanidis et al. [31], and Sanchez-Silva et al. [72], have studied the thermal decomposition of hemicellulose, in particular xylan, identifying two peaks in the DTG curve during its decomposition. The T_{m2} and T_{m3} temperature values are lower than the maximum xylan decomposition temperature found by Chen et al. [33], who reported values of 239 ºC and 280 ºC. However, as discussed in the work of Torres-Sciancalepore et al. [52], extraction processes in an acid medium produce partial hydrolysis of hemicelluloses, making them more susceptible to thermal decomposition and decreasing not only the temperature of maximum reaction rate but also the activation energy. Some authors such as Pinzi et al. (2020) and Torres-García et al. (2020), who modeled the pyrolysis of lignocellulosic biomass in multiple parallel reactions, found that hemicelluloses decompose in a single reaction stage with maximum devolatilization temperatures of 252 ºC < T_m < 262 ºC and T_m = 312 ºC, respectively.

The temperature T_{m4} corresponding to the R4 reaction may be linked to the decomposition of cellulose since the characteristic peak of cellulose decomposition in a DTG is narrow and usually located at around 330 ºC [31,33,72]. The peak with a maximum at 409 ºC corresponding to reaction R5 can be linked to the decomposition of lignin, a polymer consisting of three hydroxycinnamyl alcohol monomers differing in their degree of methoxylation: p-coumaryl, coniferyl, and sinapyl alcohols [32]. Lignin has a wide range of decomposition temperatures, although the reaction rate is usually higher at around 400 ºC [74,75]. Some authors identify multiple peaks in the DTG curve for lignin devolatilization

[33,76]. Zhou et al. [76] and Chen et al. [33] found a second peak located close to 700 ºC, which was smaller than the first, for different types of lignin. This might explain the R6 process identified in Fig. 3. On the other hand, R6 could also be explained by the decomposition of $CaCO_3$. $CaCO_3$ decomposes at around 700 °C to CaO and CO_2 [77,78]. As will be shown later in Section 3.4, RHW has high Calcium content and the ashes obtained by combustion have $Ca(OH)_2$ in them (which is formed from CaO).

The dα/dT deconvoluted curves are presented in the Supplementary Material, Fig. S4 where each reaction from R2 to R6 (Fig. 3) was isolated and considered as an independent parallel reaction. The conversion rate of each reaction is shown in Eqs. 9-13.

$$\text{R2:}\quad \frac{d\alpha_2}{dt} = 3.09\times10^{8}\text{s}^{-1}\exp\left(-\frac{84.69\,\text{kJ/mol}}{RT}\right)(1-\alpha_1)^{2.6} \tag{9}$$

$$\text{R3:}\quad \frac{d\alpha_3}{dt} = 3.63\times10^{14}\text{s}^{-1}\exp\left(-\frac{149.57\,\text{kJ/mol}}{RT}\right)(1-\alpha_2)^{4.7} \tag{10}$$

$$\text{R4:}\quad \frac{d\alpha_4}{dt} = 5.57\times10^{18}\text{s}^{-1}\exp\left(-\frac{226.37\,\text{kJ/mol}}{RT}\right)(1-\alpha_3)^{3.3} \tag{11}$$

$$\text{R5:}\quad \frac{d\alpha_5}{dt} = 1.46\times10^{13}\text{s}^{-1}\exp\left(-\frac{187.58\,\text{kJ/mol}}{RT}\right)(1-\alpha_4)^{3.9} \tag{12}$$

$$\text{R6:}\quad \frac{d\alpha_6}{dt} = 1.52\times10^{22}\text{s}^{-1}\exp\left(-\frac{421.71\,\text{kJ/mol}}{RT}\right)(1-\alpha_4)^{2.5} \tag{13}$$

Full activation energy tables with pre-exponential factors together with the master plots are presented in the Supplementary Material, Tables S5–S10 and Fig. S5.

The activation energies of R2–R6 are 84.69 kJ/mol, 149.57 kJ/mol, 226.37 kJ/mol, 187.58 kJ/mol, and 421.71 kJ/mol respectively. The activation energy of reactions R3–R5 are consistent with hemicellulose, cellulose and lignin decomposition reactions respectively, according to other authors [49,73,79]. A lower activation energy was found in R2 which may be related to extracts or a different type of hemicellulose. It was expected as well to obtain lower activation energies for hemicelluloses and cellulose as a consequence of partial hydrolysis of the polymers by the citric acid used in the extraction process [52]. On the other hand, the activation energy of pectin decomposition up to 200 °C according to Aburto et al. [71] is approximately 80 kJ/mol, which is closer to the results here presented (R2).

The activation energy of R6 is higher than that reported by Ray et al. [78] for calcite (calcium carbonate) decomposition, although it must be considered that the sample treated in this study is not pure calcite, but calcium carbonate contained inside a biomass waste. L'vov et al. [80], on the other hand, explained that there have been discrepancies in the experimental reports of the activation energy for calcite decomposition throughout the years. L'vov et al. [80] obtained an experimental result of the activation energy of calcite isobaric mode of decomposition (in the presence of excess CO_2 in the reactor atmosphere) of 493 kJ/mol which is closer to the result obtained in this work. This last assertion, as explained by L'vov et al. [80], implies that the activation energy depends on the CO_2 concentration inside the reactor.

3.4 RHW pyrolysis products analysis

The proportion released of each gaseous component during RHW pyrolysis in the fixed bed reactor as a function of temperature is shown qualitatively in Fig. 4. Each plot was drawn according to the absorbance of certain wavenumber values, characteristic of each compound,

with the exception of H_2 profile, which was obtained by calculating the area of the chromatogram peak. As may be seen, the first compounds detected by FTIR spectroscopy were CO_2 and CH_3OH, starting at 150 ºC, the temperature at which the reaction R2 is mainly in progress.

Starting at 200 ºC, CO release also begins. The process reaches maximum CO_2 and CH_3OH production at around 380 ºC and 340 ºC, respectively, coinciding with the maximum rate of cellulose devolatilization (R4). This agrees with Yang et al. [81], who found that maximum carbon dioxide release occurs between 400 ºC and 600 ºC. CO production presents a local maximum of approximately 400 ºC, followed by an increase up to 900 ºC. According to Yang et al. [81], CO production presents a local maximum between 200 ºC and 500 ºC for the pyrolysis of hemicelluloses, cellulose, and lignin, subsequently increasing again from 600 ºC onwards, especially as a consequence of the secondary pyrolysis of the tar from hemicelluloses and lignin, but also as a result of char gasification in the presence of CO_2.

Methane and ethylene production did not begin until higher temperatures: 250 ºC and 400 ºC, respectively. Maximum CH_4 production was at 630 ºC, and maximum C_2H_4 at 850 ºC, having previously reached a local maximum at 550 ºC. According to the gaseous product release profile reported by Yang et al. [81], maximum methane production occurred between 500 ºC and 600 ºC.

Hydrogen was identified in the gaseous products by GC (TCD) at two different temperature intervals. First, from 200 °C to 400 °C approximately, and later from 450 °C onwards. The maximum hydrogen release was reached at 700 °C. Yang et al. [81] found that H_2 production showed a maximum for hemicellulose, cellulose, and lignin between 650 °C and 800 °C, in agreement with the results shown in Fig. 4.

It must be emphasized the energetic importance of certain gaseous products such as H_2, CH_4, and C_2H_4. To obtain these three gases the pyrolysis temperature recommended is between 650 and 800 °C, a temperature interval at which the CO_2 emission was drastically reduced, whereas CO production was increased.

The total gas yield determined with the vertical reactor was 49.84 %, while the liquid yield (including water) was 31,26 %. These results are in agreement with the predictions of the work by Torres et al. [82], which predicts gas yields higher than 45 % for pyrolysis of lignocellulosic waste at 800 °C. It should be highlighted that at 950 °C gas yield is enhanced, whereas liquid yield starts to decrease at around 500 °C [82].

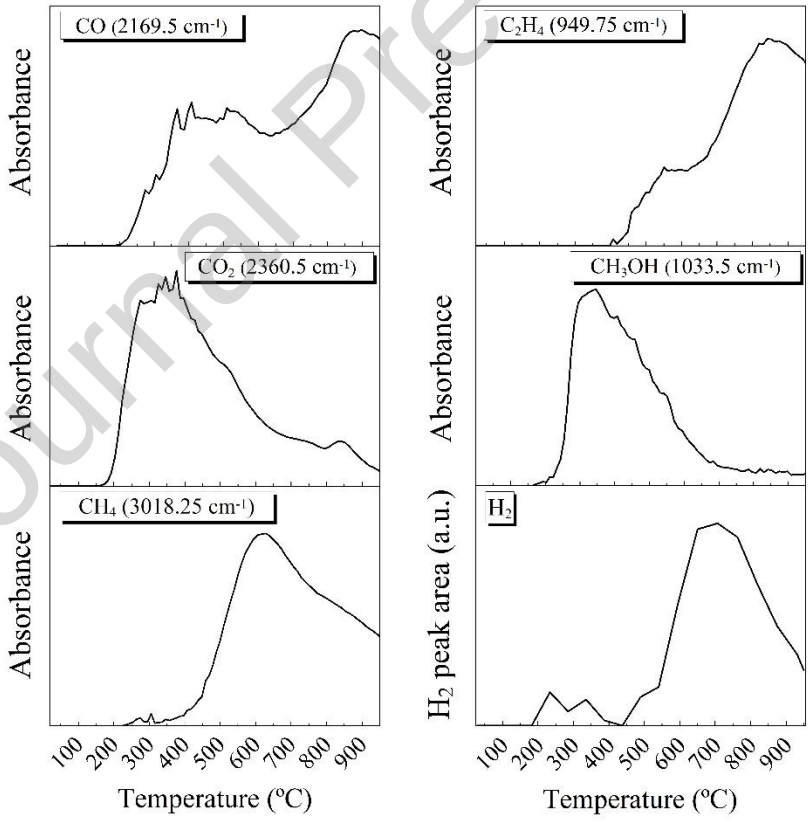

Fig. 4 Gaseous pyrolysis products absorbance detected by FTIR spectrometer and GC (hydrogen detection with TCD) at different temperatures.

The results of H_2 and CO yield analysis showed that 3.798 mmol H_2/g RHW and 2.166 mmol CO/g RHW were produced. Wang et al. [83] presented the hydrogen yield at 700 °C for slow pyrolysis of pine wood in a fixed-bed reactor with and without the presence of different catalysts. The H_2 yield reached by Wang et al. [83] in their experiment without catalyst was approximately 1.5 mmol/$g_{biomass}$, being the yield here presented higher, although it should be considered that pyrolysis experiments in this study reached a higher temperature (950 °C). H_2 production is also similar to that reported by Blanquet and Williams [84], who carried out the pyrolysis of wood pellets up to 600 °C with a two-stage pyrolysis-plasma/catalysis process obtaining a H_2 yield of 3.94 mmol/$g_{biomass}$. CO yield was lower than that presented by Wang et al. [83] without the catalyst, although it was similar to that reported by Blanquet and Williams [84] for the biomass without the pyrolysis-plasma process (only with the catalyst).

Fig. 5 shows the chromatogram for the liquid products (bio-oil) obtained at 950 ºC by pyrolysis in the fixed-bed reactor, with the names of the compounds that presented the highest peaks. Diacetone alcohol (4-hydroxy-4-methyl-2-pentanone) and mesityl oxide (4-methyl-3-penten-2-one) are most commonly used as solvents in purification processes or as precursors for the production of other substances of interest [85]. Oxacycloheptadec-10-ene-2-one is mainly found in fragrances in cosmetics, shampoos, fine fragrances, and non-cosmetic products [86], while butylated hydroxytoluene (BHT) is used as an antioxidant in cosmetic product types, dermally applied and sprayable products since it helps maintain their properties when exposed to air [87].

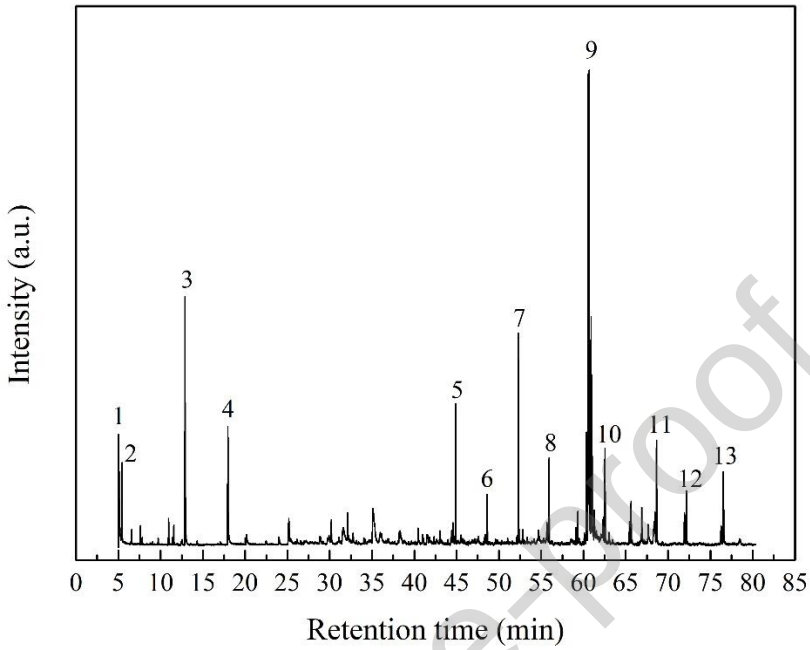

Fig. 5 Chromatogram (from GC-MS) of organic compounds found in pyrolysis bio-oil: **(1)** 4-methyl-3-penten-2-one; **(2)** 2-butanone; **(3)** 4-hydroxy-4-methyl-2-pentanone; **(4)** dihydro-3-methylene-2,5-furandione; **(5)** butylated hydroxytoluene; **(6)** hexadecane; **(7)** 2,6-dimethoxy-4-(2-propenyl)-phenol; **(8)** nonadecane; **(9)** oxacycloheptadec-10-ene-2-one; **(10)** eicosane; **(11)** heptacosane; **(12)** heneicosane; **(13)** octacosane.

Toluene, p-xylene, phenols, and naphthalene, which were also found in RHW bio-oil (presenting lower peaks), may be used as precursors for obtaining other chemicals [88]. Toluene and xylenes are used for combustion or solvents, and phenols are used in pharmaceutical industries to produce different substances such as aspirin and phenolic resins [88]. Most peaks located between a retention time of 20 and 35 min (Fig. 5) are due to phenolic-derived compounds. These phenolic and aromatic-derived compounds obtained are the result of lignin decomposition, while ketones and furan-derived molecules are mostly due to hemicelluloses and cellulose decomposition [89]. A full list of the compounds identified is available in Supplementary Material, Table S11.

The surfaces of the solids (before and after thermochemical treatment) were compared in SEM images of the raw waste and the biochar obtained at 950 ºC (see Fig. 6a and 6b). Figs. 6a.1 and 6b.1 show a 100 X magnification of RHW and biochar particles and filaments. Figs. 6a.2-3 and 6b.2-3 show a 1000 X magnification of the particles and filaments separately. It may be observed that husk particles char (Fig. 6b.2) have more pores on their surface compared to the raw particles (Fig. 6a.2) Highly porous solids are desirable in biochar when it is used as a soil amendment for contaminant removal by adsorption [34]. Additionally, a high specific surface in biochar, as a consequence of increased porosity, is of great interest for gasification reactions. On the other hand, the biochar obtained from the pyrolysis of the filaments did not present pores, though it had a rougher surface texture than the raw filaments (Fig. 6a.3). Compared to the *R. rubiginosa* rosehip seeds' char surface obtained at 950 °C shown in the work by Torres-Sciancalepore et al. [49], RHW char has lesser interstitial spaces and porosity probably reducing the available external surface. This could lead to lower reactivity to the gasification reactions of the RHW char compared to the *R. rubiginosa* rosehip seeds' char.

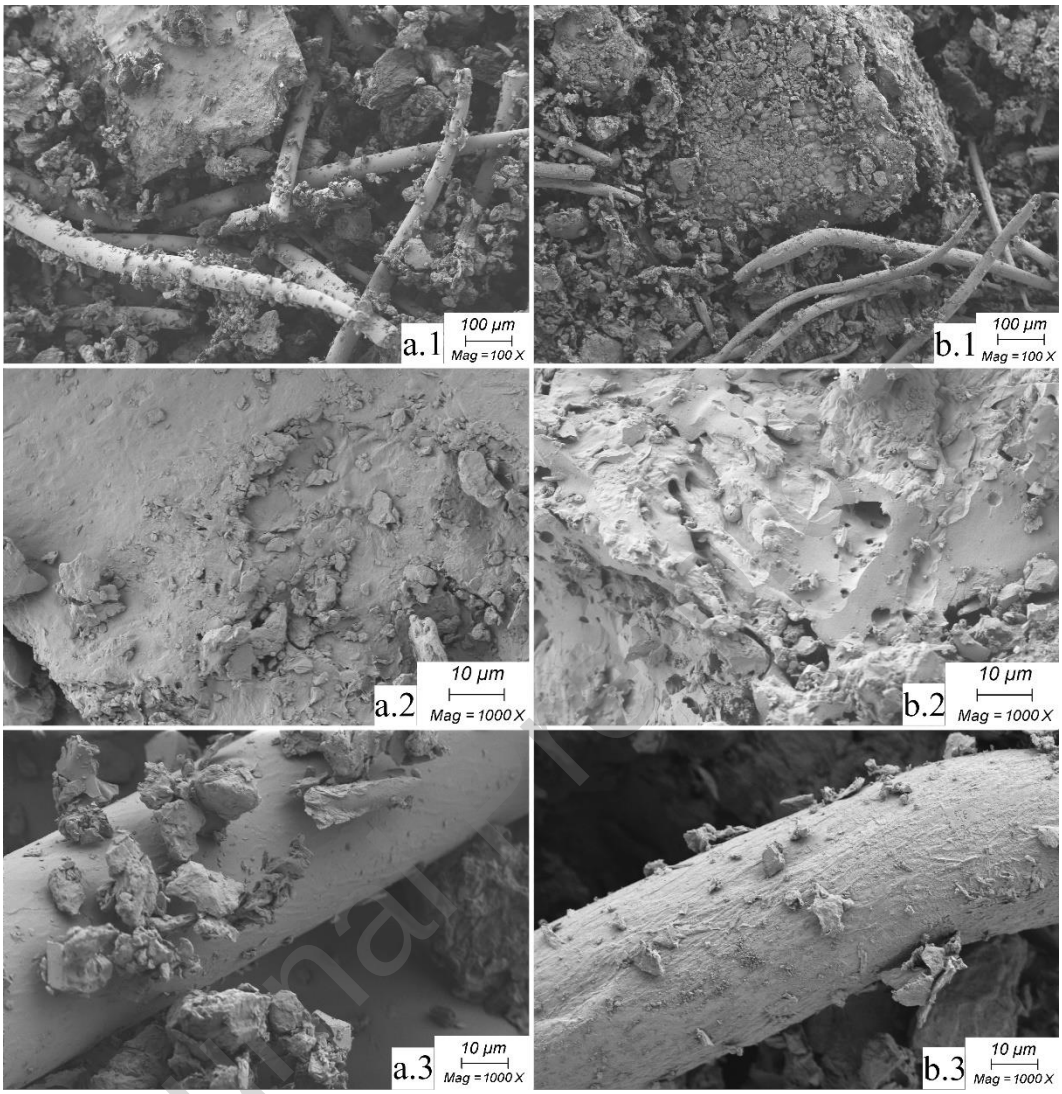

Fig. 6 SEM images of (a) raw RHW biomass and (b) 950ºC RHW char with a 100 X magnification (a.1 and b.1) and 1000 X magnification of husk particles (a.2 and b.2) and hairs (a.3 and b.3).

The main elements detected by EDS of RHW, RHW-biochar, and RHW-ash are presented in Table 3.

Table 3. EDS semi-quantitative determination of elements present in RHW, RHW char, and RHW ash.

	C (wt.%)	O (wt.%)	Ca (wt.%)	K (wt.%)	Mg (wt.%)	P (wt.%)	S (wt.%)
RHW	50.7	47	1.2	1	0.1	-	-
RHW-char	66.2	16.2	9.6	6.9	0.5	0.3	0.1

RHW-ash	3.4	39.8	43.9	8.6	2.2	1.2	0.4

As expected, the wt.% of C increased in RSW-biochar as a consequence of the carbonization process. Inorganic elements such as Ca, K, Mg, P, and S became more concentrated in the solid after pyrolysis due to the devolatilization process.

Calcium and oxygen were the predominant elements present in the RHW-ash (Table 3) and, considering the results of the XRD, it may be concluded that these elements are mostly present in the form of calcium hydroxide ($Ca(OH)_2$). Other compounds were identified by XRD as well, such as periclase (MgO) and calcium potassium phosphate ($KCaPO_4$ and $K_4Ca(PO_4)_2$). Full EDS spectra and XRD diffractogram are shown in Figs. S6–S9 in the Supplementary Material. The presence of potassium-based and calcium-based ashes promotes catalytic effects on the pyrolysis reactions of lignocellulosic biomass [90]. Lu et al. [91] demonstrated that the presence of potassium phosphate inhibits the devolatilization of hemicellulose and cellulose and promotes the decomposition of lignin to form phenolic compounds. On the other hand, Wang et al. [83] found that calcium hydroxide promotes the decomposition of cellulose and lignin constituents and enhances the yield of H_2 which is of energetic interest.

4. Conclusion

The oil production industry from rosehip seeds of the invasive species *R. rubiginosa* in Patagonia leaves the husk as residue. In the present work, the valorization of the rosehip husk was studied in two steps: an optimized eco-friendly pectin extraction, maximizing the

extraction yield and minimizing the emission of carbon dioxide, followed by a thermochemical treatment by slow pyrolysis to obtain valuable products.

After carrying out the optimization studies of the pectin extraction from RH employing the response surface method, it was found that the maximum achievable yield at the lowest possible carbon dioxide emission under the conditions analyzed was η = 17.83 % and CO_2 emission = 456.7 g CO_2/kg pectin.

Studies of RHW pyrolysis demonstrated that there is an inherent-moisture drying process followed by at least five decomposition reactions linked to the decomposition of the pseudo-components found in lignocellulosic biomass: hemicellulose, cellulose, and lignin, together with the potential decomposition of $CaCO_3$. The activation energy found in this study showed expected results for lignocellulosic pyrolysis reactions when compared with other authors. The main compounds in the tar (bio-oil) obtained by pyrolysis detected by GC-MS were diacetone alcohol, mesityl oxide, butylated hydroxytoluene, oxacycloheptadec-10-ene-2-one toluene, p-xylene, and phenol among others. Among the gaseous products carbon dioxide, carbon monoxide, methanol, methane, ethylene and hydrogen were found. The recommended pyrolysis temperature to obtain maximum methane, ethylene and hydrogen (which are of energy interest) is between 650 °C and 800 °C.

It can be concluded that the two-step process studied allows the valorization of the rosehip of the invasive species *R. rubiginosa* to obtain pectin, phenolic compounds, hydrogen, and light hydrocarbons in an eco-friendly manner. This route shows a way to make controlled use of the species, obtaining products of interest and reducing the volume of existing waste.

Acknowledgments

This research was funded by the following Argentine institutions: University of San Juan (PDTS Res. 1054/18); University of Comahue (PIN 2022–04/I260); CONICET -National Scientific and Technical Research Council (PUE PROBIEN 22920150100067 and PIP 2021–2023 -11220200100950CO); ANPCYT-FONCYT (PICT 2019-01810). Rodrigo Torres-Sciancalepore, Mathias Riveros-Gomez, and Daniela Zalazar-García have doctoral fellowships from CONICET. Maria Paula Fabani, Rosa Rodriguez, Gastón Fouga and Germán Mazza are Research Members of CONICET, Argentina.

References

[1] H. Hirsch, H. Zimmermann, C.M. Ritz, V. Wissemann, H. von Wehrden, D. Renison, K. Wesche, E. Welk, I. Hensen, Tracking the origin of invasive Rosa rubiginosa populations in Argentina, Int. J. Plant Sci. 172 (2011) 530–540. https://doi.org/10.1086/658924.

[2] T. Hura, K. Hura, M. Svriz, C. Rouco, A. Ostrowska, J. Gadzinowska, K. Urban, B. Pawłowska, Physiological and molecular features predispose native and invasive populations of sweet briar (Rosa rubiginosa L.) to colonization and restoration of drought degraded environments, Perspect. Plant Ecol. Evol. Syst. 56 (2022). https://doi.org/10.1016/j.ppees.2022.125690.

[3] J. Gadzinowska, A. Ostrowska, K. Hura, M. Dziurka, B. Pawłowska, T. Hura, Physiological traits determining high adaptation potential of sweet briar (Rosa rubiginosa L.) at early stage of growth to dry lands, Sci. Rep. 9 (2019) 1–10. https://doi.org/10.1038/s41598-019-56060-3.

[4] A.C. Mazzolari, E.N. Millán, E.M. Bringa, D.P. Vázquez, Modeling habitat suitability and spread dynamics of two invasive rose species in protected areas of Mendoza, Argentina, Ecol. Complex. 44 (2020) 100868. https://doi.org/10.1016/j.ecocom.2020.100868.

[5] D. Franco, M. Pinelo, J. Sineiro, M.J. Núñez, Processing of Rosa rubiginosa: Extraction of oil and antioxidant substances, Bioresour. Technol. 98 (2007) 3506–3512. https://doi.org/10.1016/j.biortech.2006.11.012.

[6] J.M. Quiroga, Análisis preliminar de la cadena de valor de la Rosa Mosqueta en Bariloche y zona de influencia, Argentina, SaberEs. 11 (2019) 65–80.

[7] P.M. Ramos, J.M. Gil, M.C.R. Sánchez, L.M.N. Gracia, S.H. Navarro, F.J.M. Gil, Vibrational and thermal characterization of seeds, pulp, leaves and seed oil of Rosa rubiginosa, Bol. La Soc. Argentina Bot. 51 (2016) 429–439. https://doi.org/10.31055/1851.2372.v51.n3.15388.

[8] M. Ortiz-Sanchez, J.C. Solarte-Toro, C.E. Orrego-Alzate, C.D. Acosta-Medina, C.A. Cardona-Alzate, Integral use of orange peel waste through the biorefinery concept: an experimental, technical, energy, and economic assessment, Biomass Convers. Biorefinery. 11 (2021) 645–659. https://doi.org/10.1007/s13399-020-00627-y.

[9] J.Y. Lim, S.Y. Teng, B.S. How, K.J. Nam, S.K. Heo, V. Máša, P. Stehlík, C.K. Yoo, From microalgae to bioenergy: Identifying optimally integrated biorefinery pathways and harvest scheduling under uncertainties in predicted climate, Renew. Sustain. Energy Rev. 168 (2022). https://doi.org/10.1016/j.rser.2022.112865.

[10] H.Y. Leong, C.K. Chang, K.S. Khoo, K.W. Chew, S.R. Chia, J.W. Lim, J.S. Chang, P.L. Show, Waste biorefinery towards a sustainable circular bioeconomy: a solution

to global issues, Biotechnol. Biofuels. 14 (2021) 1–15. https://doi.org/10.1186/s13068-021-01939-5.

[11] J.C. Solarte-Toro, M. Ortiz-Sanchez, C.A. Cardona Alzate, Sustainability analysis of biorefineries based on country socio-economic and environmental context: A step-by-step way for the integral analysis of biomass upgrading processes, Renew. Energy. 206 (2023) 1147–1157. https://doi.org/10.1016/j.renene.2023.02.065.

[12] M. Kiehbadroudinezhad, H. Hosseinzadeh-Bandbafha, S. Varjani, Y. Wang, W. Peng, J. Pan, M. Aghbashlo, M. Tabatabaei, Marine shell-based biorefinery: A sustainable solution for aquaculture waste valorization, Renew. Energy. 206 (2023) 623–634. https://doi.org/10.1016/j.renene.2023.02.057.

[13] G. Zoppi, E. Tito, I. Bianco, G. Pipitone, R. Pirone, S. Bensaid, Life cycle assessment of the biofuel production from lignocellulosic biomass in a hydrothermal liquefaction – aqueous phase reforming integrated biorefinery, Renew. Energy. 206 (2023) 375–385. https://doi.org/10.1016/j.renene.2023.02.011.

[14] S. Wang, Y. Mukhambet, S. Esakkimuthu, A.E.F. Abomohra, Integrated microalgal biorefinery – Routes, energy, economic and environmental perspectives, J. Clean. Prod. 348 (2022). https://doi.org/10.1016/j.jclepro.2022.131245.

[15] K. Vignesh, R. Atchaya, G. Pavan Kumar Rao, B. Shraddha, B.M. Jaffar Ali, S. Emerson Andrade, R. Arun Prasath, A.G.A. Donato, A cascaded biorefinery for the sustainable valorization of Arthrospira maxima biomass: A circular bioeconomy approach, Bioresour. Technol. Reports. 23 (2023) 101510. https://doi.org/10.1016/j.biteb.2023.101510.

[16] S. Malik, A. Shahid, M.J. Betenbaugh, C.G. Liu, M.A. Mehmood, A novel

wastewater-derived cascading algal biorefinery route for complete valorization of the biomass to biodiesel and value-added bioproducts, Energy Convers. Manag. 256 (2022) 115360. https://doi.org/10.1016/j.enconman.2022.115360.

[17] T. Haghpanah, M.A. Sobati, M.S. Pishvaee, Multi-objective superstructure optimization of a microalgae biorefinery considering economic and environmental aspects, Comput. Chem. Eng. 164 (2022) 107894. https://doi.org/10.1016/j.compchemeng.2022.107894.

[18] E. Espinosa, E. Rincón, R. Morcillo-Martín, L. Rabasco-Vílchez, A. Rodríguez, Orange peel waste biorefinery in multi-component cascade approach: Polyphenolic compounds and nanocellulose for food packaging, Ind. Crops Prod. 187 (2022). https://doi.org/10.1016/j.indcrop.2022.115413.

[19] A. Yadav, V. Sharma, M.L. Tsai, C.W. Chen, P.P. Sun, P. Nargotra, J.X. Wang, C. Di Dong, Development of lignocellulosic biorefineries for the sustainable production of biofuels: Towards circular bioeconomy, Bioresour. Technol. 381 (2023) 129145. https://doi.org/10.1016/j.biortech.2023.129145.

[20] J. Rajesh Banu, Preethi, S. Kavitha, V.K. Tyagi, M. Gunasekaran, O.P. Karthikeyan, G. Kumar, Lignocellulosic biomass based biorefinery: A successful platform towards circular bioeconomy, Fuel. 302 (2021) 121086. https://doi.org/10.1016/j.fuel.2021.121086.

[21] C. Padilla-Rascón, F. Carvalheiro, L.C. Duarte, L.B. Roseiro, E. Ruiz, E. Castro, An integrated olive stone biorefinery based on a two-step fractionation strategy, Ind. Crops Prod. 187 (2022). https://doi.org/10.1016/j.indcrop.2022.115157.

[22] C. Sabater, M. Villamiel, A. Montilla, Integral use of pectin-rich by-products in a

biorefinery context: A holistic approach, Food Hydrocoll. 128 (2022) 107564. https://doi.org/10.1016/j.foodhyd.2022.107564.

[23] V. Chandel, D. Biswas, S. Roy, D. Vaidya, A. Verma, A. Gupta, Current Advancements in Pectin: Extraction, Properties and Multifunctional Applications, Foods. 11 (2022) 1–30. https://doi.org/10.3390/foods11172683.

[24] I. Das, A. Arora, Kinetics and mechanistic models of solid-liquid extraction of pectin using advance green techniques- a review, Food Hydrocoll. 120 (2021) 106931. https://doi.org/10.1016/j.foodhyd.2021.106931.

[25] W. Wang, X. Ma, P. Jiang, L. Hu, Z. Zhi, J. Chen, T. Ding, X. Ye, D. Liu, Characterization of pectin from grapefruit peel: A comparison of ultrasound-assisted and conventional heating extractions, Food Hydrocoll. 61 (2016) 730–739. https://doi.org/10.1016/j.foodhyd.2016.06.019.

[26] M. Riveros-Gomez, D. Zalazar-García, I. Mut, R. Torres-Sciancalepore, M.P. Fabani, R. Rodriguez, G. Mazza, Multiobjective Optimization and Implementation of a Biorefinery Production Scheme for Sustainable Extraction of Pectin from Quince Biowaste, ACS Eng. Au. (2022). https://doi.org/10.1021/acsengineeringau.2c00018.

[27] S. Pedraza-Guevara, R.F. do Nascimento, M.H.G. Canteri, N. Muñoz-Almagro, M. Villamiel, M.T. Fernández-Ponce, L.C. Cardoso, C. Mantell, E.J. Martinez de la Ossa, E. Ibañez, Valorization of unripe papaya for pectin recovery by conventional extraction and compressed fluids, J. Supercrit. Fluids. 171 (2021). https://doi.org/10.1016/j.supflu.2020.105133.

[28] A.B. Kute, D. Mohapatra, N. Kotwaliwale, S.K. Giri, B.P. Sawant, Characterization

of Pectin Extracted from Orange Peel Powder using Microwave-Assisted and Acid Extraction Methods, Agric. Res. 9 (2020) 241–248. https://doi.org/10.1007/s40003-019-00419-5.

[29] Y. Zhu, T. Zhang, H. Wang, C. Zhu, M. Wei, Physicochemical properties, structure and biological activities of a novel low-molecular-weight hawthorn pectin, Process Biochem. 122 (2022) 282–291. https://doi.org/10.1016/j.procbio.2022.10.023.

[30] P. Basu, Biomass Gasification and Pyrolysis. Practical Design and Theory, First, Elsevier Inc., Burlington, 2010.

[31] S.D. Stefanidis, K.G. Kalogiannis, E.F. Iliopoulou, C.M. Michailof, P.A. Pilavachi, A.A. Lappas, A study of lignocellulosic biomass pyrolysis via the pyrolysis of cellulose, hemicellulose and lignin, J. Anal. Appl. Pyrolysis. 105 (2014) 143–150. https://doi.org/10.1016/j.jaap.2013.10.013.

[32] P. Giudicianni, G. Cardone, R. Ragucci, Hemicellulose and lignin slow steam pyrolysis : Thermal decomposition of biomass components mixtures, J. Anal. Appl. Pyrolysis. 100 (2013) 213–222. https://doi.org/10.1016/j.jaap.2012.12.026.

[33] W.H. Chen, C.F. Eng, Y.Y. Lin, Q.V. Bach, Independent parallel pyrolysis kinetics of cellulose, hemicelluloses and lignin at various heating rates analyzed by evolutionary computation, Energy Convers. Manag. 221 (2020) 113165. https://doi.org/10.1016/j.enconman.2020.113165.

[34] Y. Zhang, J. Wang, Y. Feng, The effects of biochar addition on soil physicochemical properties: A review, Catena. 202 (2021) 105284. https://doi.org/10.1016/j.catena.2021.105284.

[35] E. Sánchez, R. Zabaleta, M.P. Fabani, R. Rodriguez, G. Mazza, Effects of the

amendment with almond shell, bio-waste and almond shell-based biochar on the quality of saline-alkali soils, J. Environ. Manage. 318 (2022). https://doi.org/10.1016/j.jenvman.2022.115604.

[36] B.L. Browning, Methods of wood chemistry, Interscience publishers, New York, 1967.

[37] N. Hossain, J. Zaini, T.M.I. Mahlia, Experimental investigation of energy properties for Stigonematales sp. microalgae as potential biofuel feedstock, Int. J. Sustain. Eng. 12 (2019) 123–130. https://doi.org/10.1080/19397038.2018.1521882.

[38] K.Y. Lee, W.S. Choo, Extraction Optimization and Physicochemical Properties of Pectin from Watermelon (Citrullus lanatus) Rind: Comparison of Hydrochloric and Citric acid Extraction, J. Nutraceuticals Food Sci. 5 (2020). https://doi.org/10.36648/nutraceuticals.5.1.1.

[39] T. Happi Emaga, S.N. Ronkart, C. Robert, B. Wathelet, M. Paquot, Characterisation of pectins extracted from banana peels (Musa AAA) under different conditions using an experimental design, Food Chem. 108 (2008) 463–471. https://doi.org/10.1016/j.foodchem.2007.10.078.

[40] S.L.C. Ferreira, R.E. Bruns, H.S. Ferreira, G.D. Matos, J.M. David, G.C. Brandão, E.G.P. da Silva, L.A. Portugal, P.S. dos Reis, A.S. Souza, W.N.L. dos Santos, Box-Behnken design: An alternative for the optimization of analytical methods, Anal. Chim. Acta. 597 (2007) 179–186. https://doi.org/10.1016/j.aca.2007.07.011.

[41] Z. Raji, H. Kiani, Kinetic modeling of pectin extraction by ultrasound assisted and conventional methods, J. Food Bioprocess Eng. 3 (2020) 121–127.

[42] S.M.T. Gharibzahedi, B. Smith, Y. Guo, Ultrasound-microwave assisted extraction

of pectin from fig (Ficus carica L.) skin: Optimization, characterization and bioactivity, Carbohydr. Polym. 222 (2019) 114992. https://doi.org/10.1016/j.carbpol.2019.114992.

[43] Transparency Climate, Brown to Green: United Kingdom, (2019).

[44] T. Belwal, F. Chemat, P.R. Venskutonis, G. Cravotto, D.K. Jaiswal, I.D. Bhatt, H.P. Devkota, Z. Luo, Recent advances in scaling-up of non-conventional extraction techniques: Learning from successes and failures, TrAC - Trends Anal. Chem. 127 (2020) 115895. https://doi.org/10.1016/j.trac.2020.115895.

[45] J.M. Prado, P.C. Veggi, M.A.A. Meireles, Scale-Up Issues and Cost of Manufacturing Bioactive Compounds by Supercritical Fluid Extraction and Ultrasound Assisted Extraction, in: Glob. Food Secur. Wellness, 2017: pp. 377–433. https://doi.org/10.1007/978-1-4939-6496-3.

[46] D. Zalazar-García, G.E. Feresin, R.A. Rodriguez, Optimal operation variables of phenolic compounds extractions from pistachio industry waste (Pistacia vera var. Kerman) using the response surface method., Biomass Convers. Biorefinery. (2020). https://doi.org/10.1007/s13399-020-00862-3.

[47] S. Tripathi, R. Pandey, A. Singh, S. Mishra, Isolation and Characterisation of Value Added Product from Underutilised Part of Banana, Indian J. Sci. Technol. 14 (2021) 2317–2326. https://doi.org/10.17485/ijst/v14i28.1284.

[48] D.N.A. Zaidel, J.M. Rashid, N.H. Hamidon, L.M. Salleh, A.S.M. Kassim, Extraction and characterisation of pectin from dragon fruit (hylocereus polyrhizus) peels, Chem. Eng. Trans. 56 (2017) 805–810. https://doi.org/10.3303/CET1756135.

[49] R. Torres-Sciancalepore, D. Asensio, D. Nassini, A. Fernandez, R. Rodriguez, G.

Fouga, G. Mazza, Assessment of the behavior of Rosa rubiginosa seed waste during slow pyrolysis process towards complete recovery: Kinetic modeling and product analysis, Energy Convers. Manag. 272 (2022). https://doi.org/10.1016/j.enconman.2022.116340.

[50] C. Ma, F. Zhang, H. Liu, H. Wang, J. Hu, Thermogravimetric pyrolysis kinetics study of tobacco stem via multicomponent kinetic modeling , Asym2sig deconvolution and combined kinetics, Bioresour. Technol. 360 (2022) 127539. https://doi.org/10.1016/j.biortech.2022.127539.

[51] W. Wang, G. Luo, Y. Zhao, Y. Tang, K. Wang, X. Li, Y. Xu, Kinetic and thermodynamic analyses of co-pyrolysis of pine wood and polyethylene plastic based on Fraser-Suzuki deconvolution procedure, Fuel. 322 (2022) 124200. https://doi.org/10.1016/j.fuel.2022.124200.

[52] R. Torres-Sciancalepore, A. Fernandez, D. Asensio, M. Riveros, M.P. Fabani, G. Fouga, R. Rodriguez, G. Mazza, Kinetic and thermodynamic comparative study of quince bio-waste slow pyrolysis before and after sustainable recovery of pectin compounds, Energy Convers. Manag. 252 (2022) 115076. https://doi.org/10.1016/J.ENCONMAN.2021.115076.

[53] J.C.G. da Silva, J.G. de Albuquerque, W.V. de A. Galdino, R.F. de Sena, S.L.F. Andersen, Single-step and multi-step thermokinetic study – Deconvolution method as a simple pathway for describe properly the biomass pyrolysis for energy conversion, Energy Convers. Manag. 209 (2020) 112653. https://doi.org/10.1016/j.enconman.2020.112653.

[54] S. Vyazovkin, A.K. Burnham, J.M. Criado, L.A. Pérez-Maqueda, C. Popescu, N.

Sbirrazzuoli, ICTAC Kinetics Committee recommendations for performing kinetic computations on thermal analysis data, Thermochim. Acta. 520 (2011) 1–19. https://doi.org/10.1016/j.tca.2011.03.034.

[55] D. Paunović, A. Kalušević, T. Petrović, T. Urošević, D. Djinović, V. Nedović, J. Popović-Djordjević, Assessment of chemical and antioxidant properties of fresh and dried rosehip (Rosa canina L.), Not. Bot. Horti Agrobot. Cluj-Napoca. 47 (2019) 108–113. https://doi.org/10.15835/nbha47111221.

[56] J. Smanalieva, J. Iskakova, Z. Oskonbaeva, F. Wichern, D. Darr, Investigation of nutritional characteristics and free radical scavenging activity of wild apple, pear, rosehip, and barberry from the walnut-fruit forests of Kyrgyzstan, Eur. Food Res. Technol. 246 (2020) 1095–1104. https://doi.org/10.1007/s00217-020-03476-1.

[57] N. Ersoy, M. Salman Özen, Some Physico-Chemical Characteristics in Fruits of Rose Hip (Rosa spp.) Genotypes from Bolu Province in Western Part of Turkey, Агрознање. 17 (2017) 191. https://doi.org/10.7251/agren1602191e.

[58] R. García, C. Pizarro, A.G. Lavín, J.L. Bueno, Characterization of Spanish biomass wastes for energy use, Bioresour. Technol. 103 (2012) 249–258. https://doi.org/10.1016/j.biortech.2011.10.004.

[59] V. Dhyani, T. Bhaskar, A comprehensive review on the pyrolysis of lignocellulosic biomass, Renew. Energy. 129 (2018) 695–716. https://doi.org/10.1016/j.renene.2017.04.035.

[60] D. Zalazar-Garcia, M.C. Román, A. Fernandez, D. Asensio, X. Zhang, M.P. Fabani, R. Rodriguez, G. Mazza, Exergy, energy, and sustainability assessments applied to RSM optimization of integrated convective air-drying with pretreatments to improve

the nutritional quality of pumpkin seeds, Sustain. Energy Technol. Assessments. 49 (2022). https://doi.org/10.1016/j.seta.2021.101763.

[61] S. Sabanci, M. Çevik, A. Göksu, Investigation of time effect on pectin production from citrus wastes with ohmic heating assisted extraction process, J. Food Process Eng. 44 (2021). https://doi.org/10.1111/jfpe.13689.

[62] J. Zheng, H. Li, D. Wang, R. Li, S. Wang, B. Ling, Radio frequency assisted extraction of pectin from apple pomace: Process optimization and comparison with microwave and conventional methods, Food Hydrocoll. 121 (2021). https://doi.org/10.1016/j.foodhyd.2021.107031.

[63] I. Taneva, N. Petkova, M. Krystyjan, Characteristics and rheological properties of ammonium oxalate extracted rosehip pectin, IOP Conf. Ser. Mater. Sci. Eng. 1031 (2021). https://doi.org/10.1088/1757-899X/1031/1/012086.

[64] M. Ognyanov, C. Remoroza, H.A. Schols, Y. Georgiev, M. Kratchanova, C. Kratchanov, Isolation and structure elucidation of pectic polysaccharide from rose hip fruits (Rosa canina L.), Carbohydr. Polym. 151 (2016) 803–811. https://doi.org/10.1016/j.carbpol.2016.06.031.

[65] I. John, K. Muthukumar, A. Arunagiri, A review on the potential of citrus waste for D-Limonene, pectin, and bioethanol production, Int. J. Green Energy. 14 (2017) 599–612. https://doi.org/10.1080/15435075.2017.1307753.

[66] P. Kanmani, E. Dhivya, J. Aravind, K. Kumaresan, Extraction and Analysis of Pectin from Citrus Peels: Augmenting the Yield from Citrus limon Using Statistical Experimental Design, Iran. J. Energy Environ. 5 (2014) 303–312. https://doi.org/10.5829/idosi.ijee.2014.05.03.10.

[67] J. Luo, Y. Xu, Y. Fan, Upgrading Pectin Production from Apple Pomace by Acetic Acid Extraction, Appl. Biochem. Biotechnol. 187 (2019) 1300–1311. https://doi.org/10.1007/s12010-018-2893-1.

[68] O.A. Ijabadeniyi, Y. Pillay, Microbial safety of low water activity foods: Study of simulated and durban household samples, J. Food Qual. 2017 (2017). https://doi.org/10.1155/2017/4931521.

[69] R. Ciriminna, A. Fidalgo, R. Delisi, A. Tamburino, D. Carnaroglio, G. Cravotto, L.M. Ilharco, M. Pagliaro, Controlling the Degree of Esterification of Citrus Pectin for Demanding Applications by Selection of the Source, ACS Omega. 2 (2017) 7991–7995. https://doi.org/10.1021/acsomega.7b01109.

[70] R. Xiao, W. Yang, X. Cong, K. Dong, J. Xu, D. Wang, X. Yang, Thermogravimetric analysis and reaction kinetics of lignocellulosic biomass pyrolysis, Energy. 201 (2020) 117537. https://doi.org/10.1016/j.energy.2020.117537.

[71] J. Aburto, M. Moran, A. Galano, E. Torres-García, Non-isothermal pyrolysis of pectin: A thermochemical and kinetic approach, J. Anal. Appl. Pyrolysis. 112 (2015) 94–104. https://doi.org/10.1016/j.jaap.2015.02.012.

[72] L. Sanchez-Silva, J. Villaseñor, P. Sánchez, J.L. Valverde, Thermogravimetric – mass spectrometric analysis of lignocellulosic and marine biomass pyrolysis, Bioresour. Technol. 109 (2012) 163–172. https://doi.org/10.1016/j.biortech.2012.01.001.

[73] S. Pinzi, C. Buratti, P. Bartocci, G. Marseglia, F. Fantozzi, M. Barbanera, A simplified method for kinetic modeling of coffee silver skin pyrolysis by coupling pseudo-components peaks deconvolution analysis and model free-isoconversional

methods, Fuel. 278 (2020) 118260. https://doi.org/10.1016/j.fuel.2020.118260.

[74] E. Torres-García, L.F. Ramírez-Verduzco, J. Aburto, Pyrolytic degradation of peanut shell: Activation energy dependence on the conversion, Waste Manag. 106 (2020) 203–212. https://doi.org/10.1016/j.wasman.2020.03.021.

[75] C.M. Santos, L.S. de Oliveira, E.P. Alves Rocha, A.S. Franca, Thermal conversion of defective coffee beans for energy purposes: Characterization and kinetic modeling, Renew. Energy. 147 (2020) 1275–1291. https://doi.org/10.1016/j.renene.2019.09.052.

[76] H. Zhou, Y. Long, A. Meng, Q. Li, Y. Zhang, The pyrolysis simulation of five biomass species by hemi-cellulose, cellulose and lignin based on thermogravimetric curves, Thermochim. Acta. 566 (2013) 36–43. https://doi.org/10.1016/j.tca.2013.04.040.

[77] M. Thyrel, R. Backman, D. Boström, U. Skyllberg, T.A. Lestander, Phase transitions involving Ca – The most abundant ash forming element – In thermal treatment of lignocellulosic biomass, Fuel. 285 (2021) 119054. https://doi.org/10.1016/j.fuel.2020.119054.

[78] S. Ray, T.K. Bhattacharya, V.K. Singh, D. Deb, S. Ghosh, S. Das, Non-isothermal decomposition kinetics of nano-scale CaCO3 as a function of particle size variation, Ceram. Int. 47 (2021) 858–864. https://doi.org/10.1016/j.ceramint.2020.08.198.

[79] J. Zhang, T. Chen, J. Wu, J. Wu, A novel Gaussian-DAEM-reaction model for the pyrolysis of cellulose, hemicellulose and lignin, RSC Adv. 4 (2014) 17513–17520. https://doi.org/10.1039/c4ra01445f.

[80] B. V. L'vov, L.K. Polzik, V.L. Ugolkov, Decomposition kinetics of calcite: A new

approach to the old problem, Thermochim. Acta. 390 (2002) 5–19. https://doi.org/10.1016/S0040-6031(02)00080-1.

[81] H. Yang, R. Yan, H. Chen, D.H. Lee, C. Zheng, Characteristics of hemicellulose, cellulose and lignin pyrolysis, Fuel. 86 (2007) 1781–1788. https://doi.org/10.1016/j.fuel.2006.12.013.

[82] E. Torres, L.A. Rodriguez-Ortiz, D. Zalazar, M. Echegaray, R. Rodriguez, H. Zhang, G. Mazza, 4-E (environmental, economic, energetic and exergetic) analysis of slow pyrolysis of lignocellulosic waste, Renew. Energy. 162 (2020) 296–307. https://doi.org/10.1016/J.RENENE.2020.07.147.

[83] Z. Wang, F. Wang, J. Cao, J. Wang, Pyrolysis of pine wood in a slowly heating fixed-bed reactor: Potassium carbonate versus calcium hydroxide as a catalyst, Fuel Process. Technol. 91 (2010) 942–950. https://doi.org/10.1016/j.fuproc.2009.09.015.

[84] E. Blanquet, P.T. Williams, Biomass pyrolysis coupled with non-thermal plasma/catalysis for hydrogen production: Influence of biomass components and catalyst properties, J. Anal. Appl. Pyrolysis. 159 (2021) 105325. https://doi.org/10.1016/j.jaap.2021.105325.

[85] S. Thotla, V. Agarwal, S.M. Mahajani, Simultaneous production of diacetone alcohol and mesityl oxide from acetone using reactive distillation, Chem. Eng. Sci. 62 (2007) 5567–5574. https://doi.org/10.1016/j.ces.2007.01.045.

[86] D. McGinty, C.S. Letizia, A.M. Api, Fragrance material review on oxacycloheptadec-10-ene-2-one, Food Chem. Toxicol. 49 (2011) S189–S192. https://doi.org/10.1016/j.fct.2011.07.025.

[87] B. Granum (rapporteur), U. Bernauer, L. Bodin, Q. Chaudhry, C. Pieter Jan, M.

Dusinska, J. Ezendam, E. Gaffet, C.L. Galli, E. Panteri, V. Rogiers, C. Rousselle, M. Stepnik, T. Vanhaecke, S. Wijnhoven, A. Koutsodimou, W. Uter, N. von Goetz, SCCS scientific opinion on Butylated hydroxytoluene (BHT) - SCCS/1636/21, Regul. Toxicol. Pharmacol. 138 (2023) 2022–2023. https://doi.org/10.1016/j.yrtph.2022.105312.

[88] S. Matar, L.F. Hatch, Chemicals Based on Benzene, Toluene, and Xylenes, Chem. Petrochemical Process. (2001) 262–300. https://doi.org/10.1016/b978-088415315-3/50011-0.

[89] S. Wang, X. Guo, K. Wang, Z. Luo, Influence of the interaction of components on the pyrolysis behavior of biomass, J. Anal. Appl. Pyrolysis. 91 (2011) 183–189. https://doi.org/10.1016/j.jaap.2011.02.006.

[90] W. Wang, R. Lemaire, A. Bensakhria, D. Luart, Review on the catalytic effects of alkali and alkaline earth metals (AAEMs) including sodium, potassium, calcium and magnesium on the pyrolysis of lignocellulosic biomass and on the co-pyrolysis of coal with biomass, J. Anal. Appl. Pyrolysis. 163 (2022) 105479. https://doi.org/10.1016/j.jaap.2022.105479.

[91] Q. Lu, Z.B. Zhang, X.C. Yang, C.Q. Dong, X.F. Zhu, Catalytic fast pyrolysis of biomass impregnated with K3PO 4 to produce phenolic compounds: Analytical Py-GC/MS study, J. Anal. Appl. Pyrolysis. 104 (2013) 139–145. https://doi.org/10.1016/j.jaap.2013.08.011.

Graphical abstract

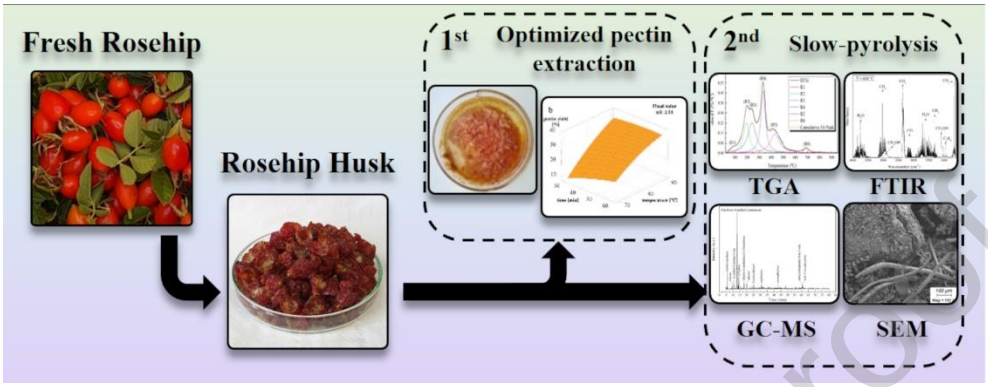

CRediT authorship contribution statement

Rodrigo Torres-Sciancalepore: Conceptualization, Formal analysis, Investigation, Writing - original draft, Software.

Mathias Riveros-Gomez: Conceptualization, Formal analysis, Investigation, Writing - original draft, Software.

Daniela Zalazar-García: Conceptualization, Formal analysis, Software.

Daniela Asensio: Conceptualization, Methodology, Investigation, Formal analysis.

María Paula Fabani: Conceptualization, Methodology, Investigation, Funding acquisition.

Rosa Rodriguez: Conceptualization, Resources, Writing - review & editing, Supervision, Project administration, Funding acquisition.

Gastón Fouga: Conceptualization, Investigation, Formal analysis, Writing - review & editing, Supervision, Resources.

Germán Mazza: Formal analysis, Visualization, Resources, Writing - review & editing, Supervision, Project administration, Funding acquisition.

Declaration of interests

☒ The authors declare that they have no known competing financial interests or personal relationships that could have appeared to influence the work reported in this paper.

☐The authors declare the following financial interests/personal relationships which may be considered as potential competing interests:

Highlights

- Optimal pectin extraction conditions were at T=79.6 ºC, t=30 min, and pH=2.3
- Maximum pectin yield and minimum CO_2 emission were 17.83 % and 456.7 g_{CO_2}/kg_{pectin}
- Six steps were identified by deconvolution of DTG in the pyrolysis of rosehip husk
- Maximum CH_4, C_2H_4 and H_2 production by pyrolysis was between 650 °C and 800 °C
- Rosehip husk ash showed a high Ca concentration (46.9 %) forming $Ca(OH)_2$ and $KCaPO_4$